INL/JOU-23-72162-Revision-0

Evaluation of artificial neural network performance for classification of potato plants infected with potato virus Y using spectral data on multiple varieties and genotypes

L. Michael Griffel, Donna Delparte, Jonathan Whitoworth, Paul Bodily, Damon S Hartley

Changing the World's Energy Future

Idaho National Laboratory

INL is a U.S. Department of Energy National Laboratory operated by Battelle Energy Alliance, LLC

INL/JOU-23-72162-Revision-0

Evaluation of artificial neural network performance for classification of potato plants infected with potato virus Y using spectral data on multiple varieties and genotypes

L. Michael Griffel, Donna Delparte, Jonathan Whitoworth, Paul Bodily, Damon S Hartley

February 2023

Idaho National Laboratory
Idaho Falls, Idaho 83415

http://www.inl.gov

Prepared for the
U.S. Department of Energy
Under DOE Idaho Operations Office
Contract DE-AC07-05ID14517

Smart Agricultural Technology 3 (2023) 100101

Contents lists available at ScienceDirect

Smart Agricultural Technology

journal homepage: www.journals.elsevier.com/smart-agricultural-technology

Evaluation of artificial neural network performance for classification of potato plants infected with potato virus Y using spectral data on multiple varieties and genotypes

L.M. Griffel [a,*], D. Delparte [a], J. Whitworth [b], P. Bodily [c], D. Hartley [d]

[a] Department of Geosciences, Idaho State University, 921 S 8th Ave, Pocatello, Idaho, 83209-8072, USA
[b] United States Department of Agriculture Agricultural Research Service, Small Grains and Potato Germplasm Research, 1693 S 2700W, Aberdeen, Idaho, 83210, USA
[c] Department of Computer Science, Idaho State University, 921 S 8th Ave, Pocatello, Idaho, 83209-8072, USA
[d] Bioenergy Technologies, Modelling and Simulation, Idaho National Laboratory, P.O. Box 1625, Idaho Falls, Idaho, 83415, USA

ARTICLE INFO

Keywords:
Potato Virus Y
Machine learning
Remote sensing
Spectrometry
Artificial neural networks

ABSTRACT

Potato virus Y (*Potyviridae*, PVY) is a plant virus that poses a significant threat to potato producers on a global basis. The pathogen has disrupted seed potato supplies and negatively impacted yield and quality of commercial potato crops. The potato industry currently manages PVY infection levels via insecticide applications, regional seed certification programs that rely on field scouting to visually assess individual plants for infection status, and destructive and costly tissue sampling coupled with laboratory assays. Despite these efforts, PVY continues to confound potato industry stakeholders resulting in economic harm. Remote sensing and machine learning provide for the development of new tools to more accurately detect and spatially quantify PVY-infected plants versus the current state of the art. However, there is a need to understand how the occurrence of many different potato varieties impact the dynamics of developing models to detect potato plants impacted with PVY and their potential effectiveness. This study evaluates classification modelling outcomes using spectral datasets collected in different temporal and spatial environments (greenhouse and a production field) on multiple potato varieties consisting of labelled instances of plants infected with PVY and those not infected with the virus. A modelling framework was developed to support iterative modelling runs using artificial neural network (ANN) architectures configured as binary classifiers to develop sample populations to support statistical analysis on model performance using specific spectral subsets. When using spectral data to detect PVY-infected plants, ANN models achieved the highest mean accuracy of 0.894 on a single variety. Conversely, the same ANN model architecture only achieved a mean accuracy of 0.575 on a spectral data set representing 29 potato breeding lines. Additionally, statistical analysis indicates spectral regions including the red edge, near infrared and shortwave infrared contain more important spectral features for the ANN classifier introduced in this research.

1. Introduction

Potato *(Solanum tuberosum)* ranks as the third most important food crop relative to global human consumption and supplies over 1 billion consumers while contributing to food security and agricultural resilience [4]. As an agricultural crop, many nations have expanded potato production capacity over the past 20 years driven by significant increases in China and India [49]. In the United States, potato production surpassed 369,920 ha in 2020 with an estimated value of $3.9 billion (https://www.nationalpotatocouncil.org/). In addition to being an important food source, a portion of harvested acres are reserved for potato seed production since the vast majority of potato crops rely on vegetative reproduction. Potato production using true botanical seed is rare since resultant individual plants within a field are genetically heterogenous and can produce tubers of varying size, shape, colour, and other attributes [42]. Vegetative reproduction results in a genetically homogenous crop yielding tubers with uniform characteristics necessary to support food manufacturing supply chains. However, seed tubers used for vegetative reproduction can serve as sources of inoculum for multiple plant diseases with potential to damage subsequent potato crop yields and quality [33].

Potato virus Y (*Potyviridae*, PVY) was first recognized in the early

* Corresponding author.
E-mail addresses: griffloy@isu.edu (L.M. Griffel), delparte@isu.edu (D. Delparte).

https://doi.org/10.1016/j.atech.2022.100101
Received 18 April 2022; Received in revised form 29 July 2022; Accepted 31 July 2022
Available online 1 August 2022

Fig. 1. A Russet Norkotah potato plant (Centre) showing visual symptoms of PVY infection in an agricultural production field in eastern Idaho during the summer growing season. Symptoms include slightly stunted growth, rough and crinkled leaf texture, and a slightly different green hue in overall plant colour. (Photo taken by L.M. Griffel in June 2015).

1930s [40] and has been ranked fifth among the top ten most economically important plant viruses due to its deleterious impacts on yield and marketability [39]. PVY is a single-strand RNA virus that is often classified into biological strains including PVY^{O}, PVY^{N}, PVY^{C}, $PVY^{N:O}$, $PVY^{N\text{-}Wi}$, and PVY^{NTN} [18]. Analysis of the phylodynamics of PVY indicate the virus originated in South America and was transported to Europe in the 19th century and subsequently to other regions around the globe [8, 43]. Multiple aphid species have been shown to be an important in-season vector for PVY including *Brachycaudus helichrysi, Myzus persicae, Phorodon humuli, Aphis* species, and *B. helichrysi* [15,25, 28–30,45]. Potato seed tubers, either intentionally cultivated and harvested or those promulgated through volunteer plant populations that result from un-harvested tubers, can harbour PVY from one growing season to the next [13]. Mondal et al. [31] assessed mixed PVY strain dynamics in three potato varieties and found that PVY^{O} and PVY^{NTN} strains can accumulate simultaneously in daughter tubers after infecting mother plants. Yield losses due to PVY have been documented to be as high as 79 percent in field trials and can result in significant internal and/or external tuber defects depending upon potato variety and biological disease strain [11,14]. Nolte et al. [34] documented economic losses ranging from $16.96/ha to $17.91/ha for each percentage of increase in PVY at a field level across multiple varieties and growing seasons.

Current efforts to control the spread of PVY are focused on the development and maintenance of clean potato seed production systems, often managed by state or regional potato seed certification programs with regulatory authority. Within these programs, seed potato crops are subjected to intense in-season field scouting and post-harvest tissue sampling coupled with laboratory assays that are intended to quantify disease incidence to rate potato seed lots [22,50]. In turn, these regulatory steps compel seed producers to take steps to minimize disease buildup in seed stocks to maintain marketability. Seed potato growers try to spatially isolate fields to limit exposure of neighbouring crops with potentially higher incidences of PVY along with regular applications of pesticides to reduce insect vectors and manually remove (rogue) infected plants and tubers based on visual symptoms [6,11]. Visual foliage cues of plants infected with PVY can vary depending upon the potato cultivar, PVY strain, environmental and crop agronomic conditions, and other factors making accurate detection difficult without proper training and experience [18]. In many cases, foliage symptoms can include a mosaic pattern of green and yellow tissue, rough and crinkled leaf texture, small necrotic lesions, stunted growth, and a slightly different green hue as shown in Fig. 1.

Conventional breeding in the U.S. has led to new varieties such as Payette Russet [35] and Eva [36] with PVY resistance conferred by the *Ry* gene. The resulting resistance has been shown to be effective against PVY strains O, N:O, NTN, and N-Wi in these and other varieties [47,48]. While this conventionally bred resistance is available, the resistant varieties are not yet widely grown. Additionally, given PVY mixed-strain infection dynamics in multiple potato varieties documented by Mondal [31], there is potential for PVY genetic mutations to outpace conventionally bred resistance.

Despite significant efforts to meet seed potato certification standards, accurately detecting, quantifying, and reducing PVY in seed potatoes has not been an easy task and certification programs, potato growers, and other industry stakeholders continue to struggle with increased disease pressure and, at times, the loss of seed supplies [3,50]. In North America, PVY infection is the most common reason for downgrading or rejecting seed lots [13]. Seed certification programs managed by Idaho, Montana, and Wisconsin were shown to have significant discrepancies between PVY levels measured during in-season field inspections and post-harvest laboratory testing highlighting the current limitations of accurately detecting and quantifying PVY incidence [38]. The discrepancies exist because in-field testing doesn't capture all the virus transmission that can occur between the test and harvest time. Because the industry depends primarily on visually assessing PVY symptoms to guide management and certification decisions and costly destructive tissue sampling coupled with laboratory assays, the opportunity exists for the development of robust, accurate, and high-throughput detection algorithms that incorporates remote sensing data and machine learning (ML) to improve disease verification and removal strategies.

A growing body of work indicates remote sensing of electromagnetic (EM) reflectance coupled with classification via ML algorithms can achieve high accuracies when it comes to in-situ detection of potato plants infected with PVY based on spectral foliage characteristics. This type of application represents a significant improvement over current

Fig. 2. The field spectrometer equipment setup for data collection in the greenhouse environment.

time-consuming and labour-intensive field sampling protocols coupled with destructive laboratory-based characterization assays. Griffel et al. [12] utilized Support Vector Machines (SVM) classification to differentiate PVY-infected potato plants within a potato production field based on EM reflectance measured by a field spectrometer achieving accuracies of almost 90 percent by utilizing red edge and near infrared (NIR) spectral regions. Analysis of spectroradiometer data has shown that partial-least squares discriminate analysis can differentiate asymptomatic potato leaves from PVY-infected plants from those of non-infected plants and that shortwave infrared (SWIR) spectral regions displayed the strongest correlation with infection status [2]. The research also provided insights on plant biochemical and physiological properties indicating that PVY infection slightly increased leaf lignin content and decreased photosynthetic capacity. Polder et al. [37] demonstrated high precision and recall metrics when applying convolutional neural network (CNN) architectures to detect PVY-infect potato plants using hyperspectral imagery. The authors claim CNN model precision was almost equal to an experienced crop expert trained to recognize PVY foliage symptoms. Spectral data from two potato varieties were evaluated by Moslemkhani et al. [32] using principal components analysis (PCA) for PVY detection. Specifically, the PCA loading weights indicated that the spectral range of 900 to 1100 nm was most sensitive to PVY infection. Linear discriminant analysis was applied to selected spectral data from the subset region and achieved classification results with high accuracy.

Although previous analysis has demonstrated high classification accuracies for PVY detection using spectral data, additional work is needed to better understand the impacts of multiple potato varieties on models designed to classify PVY-infected potato plants from non-infected counterparts. The literature contains multiple sources (previously noted) that indicate visual symptoms of PVY infection vary by potato variety with some showing strong leaf texture, colour, and plant size differences while others express mild to no visual cues. The goal of this study is to develop, train, and test supervised artificial neural network (ANN) models implemented as densely connected feedforward multilayer perceptron (MLP) models using spectral reflectance data collected from multiple potato varieties and genotypes to answer whether or not a single model is capable of accurate classification using only spectral data across multiple potato varieties and genotypes. Additional statistical analysis will be utilized to explore if specific spectral subsets contribute to improved ANN performance. ANNs were selected for this analysis as they can solve non-linear complex classification tasks without having to explicitly define the complex relationships within the feature space, something typically required by traditional statistical techniques [9]. CNNs are not appropriate for this specific type of spectral data as they are not collected on a pixel-basis. Model tests will be used to quantify important performance metrics including accuracy, precision, and recall. For this analysis, spectral data quantifying EM reflectance from PVY-infected and non-infected plants were collected with a field spectrometer from greenhouse and production field environments. Spectral data are an effective tool to measure and characterize EM reflectance [26]. The following sections of this paper are structured as follows. Section 2 will detail the data and associated collection methods, algorithm development, classification modelling, and statistical analysis. Section 3 will show all results followed by discussion points and conclusion statements in sections 4 and 5, respectively.

2. Materials and methods

2.1. Data

To support this analysis, two spectral datasets were compiled that were collected with a FieldSpec 4 spectroradiometer (Analytical Spectral Devices, a PANalytical Company, Longmont, CO, USA). The data consists of EM reflectance values (floating values ranging from 0 to 1) at

Table 1
Spectral region subsets.

Spectral Range (nm)	Number of Features	Description
380–720	340	Blue, Green, and Red
500–900	400	Green, Red, Red Edge, and NIR
720–900	180	Red Edge and NIR
720–1300	580	Red Edge, NIR, and SWIR
900–1300	400	NIR and SWIR

a 1-nm resolution for wavelengths ranging from 350 to 2500 nm totalling 2151 spectral features. The first spectral dataset was collected in 2015 at an agricultural potato production field in southeastern Idaho, United States which was planted to the Russet Norkotah variety. The grower/cooperator requested that the specific geographical coordinates not be published for anonymity. This effort was detailed by Griffel et al. [12] and will only be highlighted here. Researchers identified 31 plants infected with PVY based on visual symptoms and confirmed the presence of the virus using enzyme-linked immunosorbent assays (ELISA). The specific PVY strains were identified using Immunocapture Multiplex Reverse Transcriptase Polymerase Chain Reaction (RT-PCR) revealing the presence of PVY^{NTN}, $PVY^{N:O}$, and PVY^{O}. Additionally, an equal number of control plants not infected with PVY were identified. Spectral data were collected from each plant at a minimum of three times during the growing season resulting in 242 spectral scans evenly balanced between infected and non-infected instances. All scans were collected by positioning the sensor directly above the plant at a distance of 100–150 mm to minimize any background soil reflectance. The spectrometer was optimized before each data collection campaign and continually calibrated using a Spectralon white target any time light conditions changed. This provided a dataset where every spectral instance was collected from a single potato variety and will be referred to as the *Single Variety* dataset. It is important to note that the results detailed here differ from the analysis results presented by Griffel et al. [12] as different modelling techniques were used for this classification analysis.

A second spectrometer dataset was collected at the United States Department of Agriculture Agricultural Research Service (USDA-ARS) Small Grains and Potato Germplasm Research greenhouse facility in Aberdeen, Idaho, United States in 2016. In this case, the data were collected with the same instrument used by Griffel et al. [12] from a potato breeding program with a heterogeneous mixture of genetic entries (breeding lines) with confirmed PVY-infections. The field spectrometer was optimized at the beginning of each data collection period and calibrated approximately every 20 min during the collection run to account for any changes in light conditions. A supplementary halogen axial filament light source was mounted above the scanned target area. All scans were taken directly above infected plants at an approximate distance of 100–150 mm from the sensor to minimize any background reflectance effects as shown in Fig. 2.

Each plant sample belonged to one of 38 different variety breeding line entries developed by the program and was scanned inside the greenhouse production system on four dates during the growing cycle (February 17, 2016, February 24, 2016, March 2, 2016, and March 9, 2016). Multiple entries and dates are represented in the data. ELISA results used to determine virus presence in plant materials were compiled for each plant providing infection status. Additional testing using RT-PCR revealed the presence of PVY^{NTN} and $PVY^{N:O}$ strains. Observations of non-virus symptoms on the leaves that may contribute bias to the spectral imaging were noted to support data selection decisions for modelling efforts to ensure that spectral data used were clear of confounding symptoms. Additionally, since the number of instances of PVY-infected and non-infected was not always balanced within the individual breeding lines, random sub-setting was performed to develop a balanced dataset where each breeding line was balanced. These data present an opportunity to evaluate EM reflectance from potato plant foliage tissue across a multitude of varieties genetic backgrounds than can exhibit significantly different phenotypic responses relative to plant foliage structure and colour and will be referred to as the *Multiple Varieties* dataset.

Given the large number of features (2151 spectral wavelengths) present in the spectral data, it was decided to subset the data into smaller spectral regions as defined by Griffel et al. [12]. This would allow for analysis to better understand if some spectral regions contained features more important for ANN classification for PVY-infected potato plants. Table 1 shows the spectral ranges used in this analysis.

2.2. ANN modelling

For classification using the spectral data, ANN model architectures were developed as feedforward densely connected MLPs consisting of input, hidden, and output layers. This work was performed using Python 3.6 and the TensorFlow 2.1 software package [1,44]. A common ANN structure was developed to classify each dataset derived from the field and greenhouse efforts independently for comparison purposes. The model structure, shown in Fig. 3, consisted of a flexible input layer (to accommodate for varying input features) followed by hidden layers with 1200, 800, 400, 200, 50, 10 neurons respectively. Each hidden layer was configured with a rectified linear unit (ReLU) activation function [10] shown by Eq. (1):

$$f(x) = \begin{cases} 0, x < 0 \\ x, x \geq 0 \end{cases} \quad (1)$$

where $f(x)$ is always positive and x, the neuron input, is not bounded in the positive direction. This activation function is commonly used as it converges faster, x does not plateau or saturate in the positive direction, and it is sparsely activated as all negative inputs are converted to zero within the network. The models were optimized with the Adam function [20] using learning a learning rate of 0.000001. Adam is a stochastic-gradient-based optimization method favored for its computational efficiency and straightforward implementation based on intuitive hyper-parameters that require little tuning. The output layer was

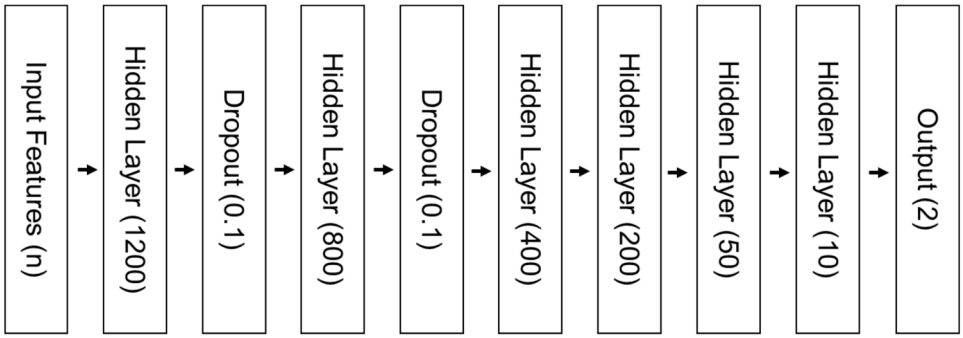

Fig. 3. The ANN model structure used for the classification analysis.

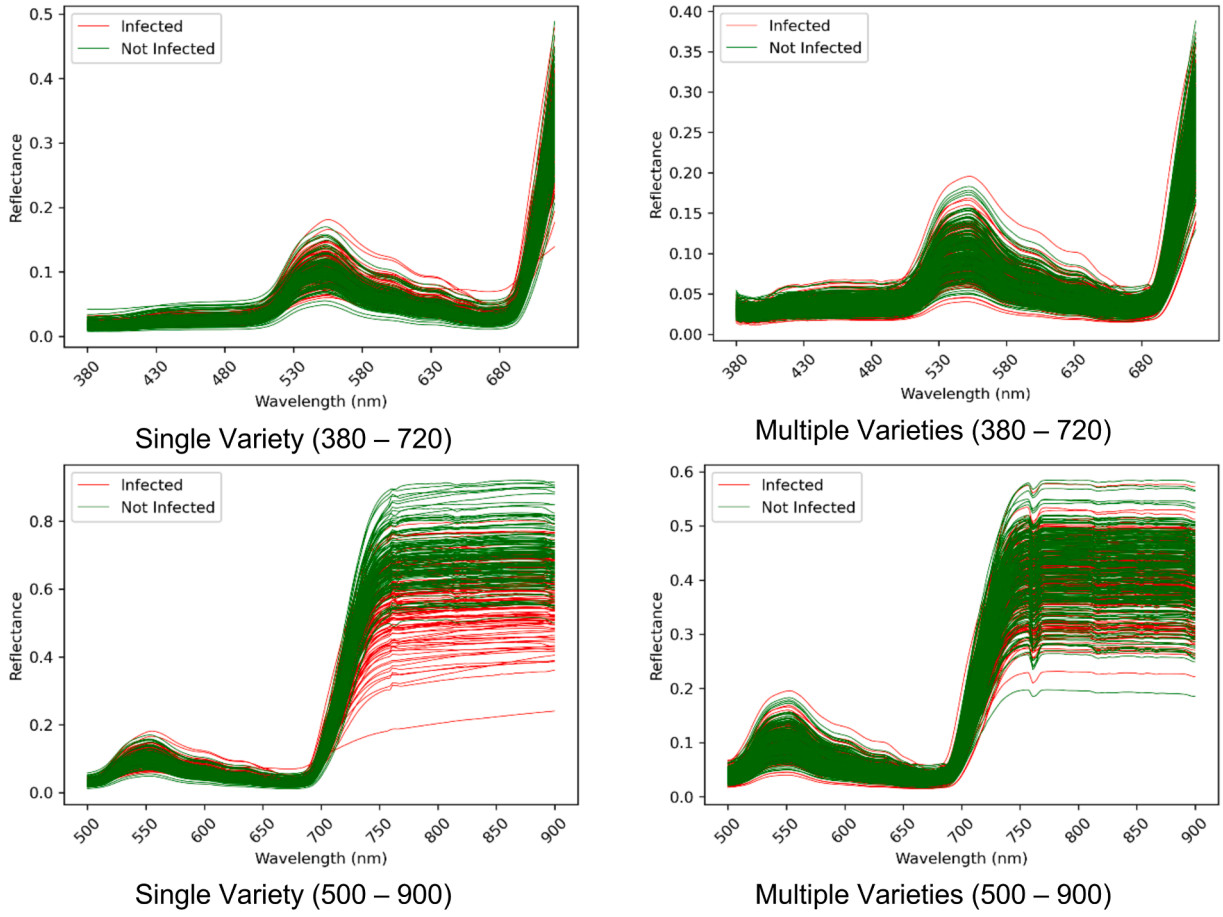

Fig. 4. Plots of the spectral subset features for the Single Variety (left) and Multiple Varieties (right) datasets used as inputs for the ANN modelling analysis. The green lines represent "Not Infected" plants, and the red lines represent "Infected" plants.

configured with two neurons (representing "Infected" and "Not Infected" classes) and configured with the softmax activation function that can be interpreted as a probability distribution representing the model's output decision. Additionally, given that the number of input instances are relatively small (i.e. 242 instances within the field data), dropout layers [41] were added after the first and second hidden layers to reduce the risk of overfitting.

In many classification analyses, researchers report singular accuracy metrics based upon a randomized split of the data instances into training and testing groups. This makes sense when the number of instances is sufficient to have reasonable confidence that the input features adequately represent the expected distributions after the train-test split. However, when restricted to a relatively small number of instances due to limitations of data collection, there is a risk that the training data may not include an adequate representation of the feature space distribution which could impede model performance. This is further confounded when an additional subset is required from the data for model validation during training. To address this risk, a modelling framework was developed to support an iterative approach to define model performance distributions versus singular metrics. Each dataset (Single Variety and Multiple Varieties) was randomly split into training and testing groups (proportions of 0.8 and 0.2 respectively) for 100 iterations for each spectral feature subset shown in Table 1. Within each iteration, a model structured as shown in Fig. 3 was instantiated and trained on a training group. Within the training group, a second random subset (proportion of 0.1) was selected for validation to track for model overfitting during training. Validation accuracy and loss were calculated on the validation subset at the end of each training epoch. Accuracy was calculated as the ratio of correct inferences over in-correct inferences and model loss was calculated with a categorical cross entropy function. Model training was terminated when the model loss metrics failed to improve for 100 epochs. The trained model that achieved the lowest loss function output on the validation data was then tasked to infer on the appropriate testing group which provided the final accuracy, precision, and recall metrics. Precision and recall are calculated as shown in Eqs. (2) and (3):

$$Precision = \frac{TP}{TP + FP} \tag{2}$$

$$Recall = \frac{TP}{TP + FN} \tag{3}$$

where *TP* represents true positive inferences, *FP* represents false positive inferences and *FN* represents false negative inferences.

2.3. Statistical analysis

After the modelling framework analysis, the iteration results were compiled and served as sample populations for statistical tests to investigate if statistically significant differences existed in the model inferences for each spectral subset of input features within each dataset. The statistical analyses were conducted with the SciPy software package for Python [46]. A Shapiro-Wilks Test [27] was applied to the accuracy, precision, and recall metrics to determine if each approximated a normal distribution–this is necessary as some statistical tests require an assumption of normally distributed data. The Shapiro-Wilks test rejects the null hypothesis (H_0) of normality when the probability value is less

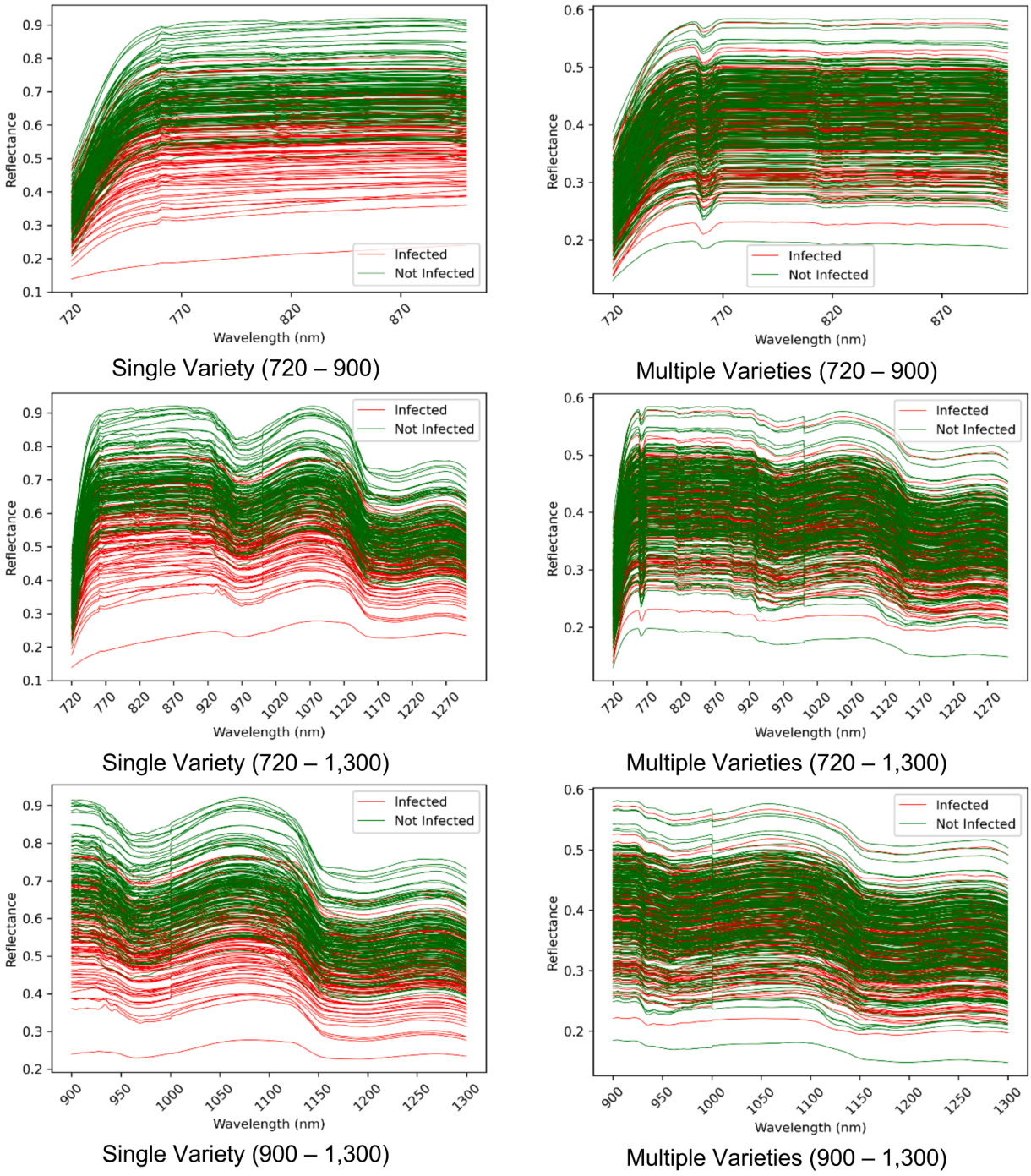

Fig. 4. (*continued*).

than a selected threshold, which for this analysis was 0.05 for all statistical tests requiring a probability threshold.

Following the normality testing, the accuracy distributions of each spectral group within the individual datasets were tested for equivalence. If the normality test H_0 could not be rejected on all accuracy distributions, an Analysis of Variance (ANOVA) Test [19] was applied. In ANOVA, the null hypothesis states that there is no difference among the group means. If the normality test H_0 could be rejected on any of the model accuracy distributions, a Kruskal-Wallis Test [21] was used to evaluate the equivalence of model performance for each spectral dataset. A Kruskal-Wallis Test does not require normally distributed data distributions and poses the null hypothesis that the samples were drawn from the same population with the same median.

If the accuracy distributions among the spectral subsets for each dataset were shown to be statistically different, additional post-hoc pair-wise testing was applied to identify which model accuracy distributions of the spectral subsets were statistically different from others. Again, if the data proved normally distributed, a Tukey's Honestly Significant Difference (HSD) Test [16] was applied for the pair-wise analysis. If the Shapiro-Wilks H_0 could be rejected for any of the accuracy distributions, then a post-hoc pair-wise Dunn's Test [5] was conducted to differentiate the modelling accuracy distributions among each dataset's spectral subsets. A Dunn's Test is non-parametric and does not assume data normality and is an alternative to Tukey's HSD Test. It poses a null hypothesis that there is no difference between a given pair of groups.

Analysis was also conducted to evaluate if precision and recall

Table 2
Descriptive statistics of the modelling framework accuracy metrics.

Data	Spectral Subset	Training Epochs (mean)	Acc. (mean)	Acc. (std)	Prec. (mean)	Prec. (std)	Recall (mean)	Recall (Std)
Single Variety	380–720	902.0	0.837	0.085	0.868	0.104	0.814	0.105
	500–900	681.8	0.891	0.041	0.905	0.057	0.880	0.065
	720–900	838.8	0.894	0.039	0.901	0.052	0.889	0.067
	720–1300	928.0	0.874	0.051	0.873	0.063	0.881	0.069
	900–1300	857.1	0.856	0.050	0.852	0.062	0.867	0.075
Multiple Varieties	380–720	196.5	0.500	0.042	0.504	0.110	0.484	0.269
	500–900	254.7	0.531	0.050	0.534	0.091	0.476	0.234
	720–900	266.7	0.517	0.047	0.526	0.095	0.408	0.255
	720–1300	395.9	0.574	0.059	0.598	0.089	0.532	0.199
	900–1300	418.2	0.575	0.057	0.608	0.091	0.503	0.192

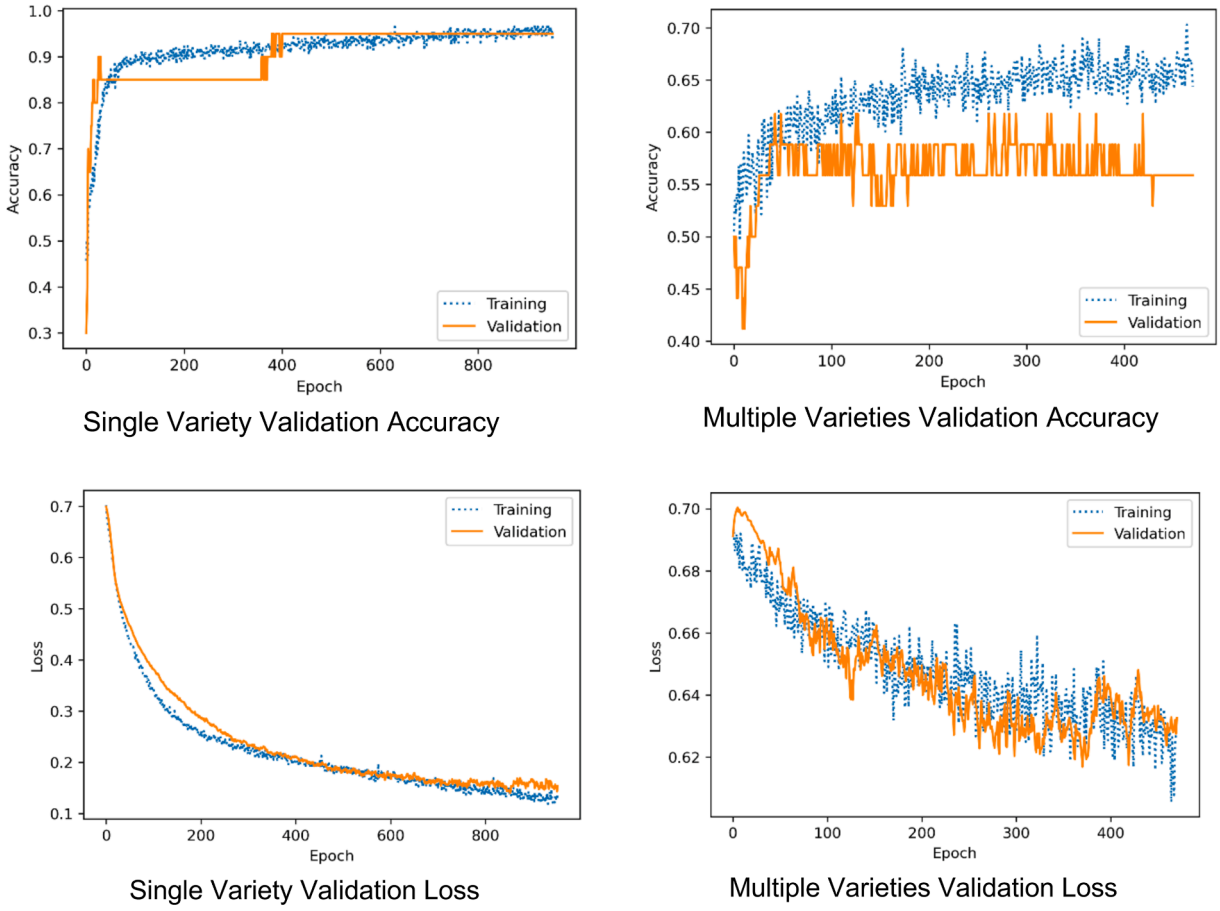

Fig. 5. Plots showing examples of validation accuracy and loss metrics during model training for Single Variety data (left) and Multiple Varieties data (right).

statistically differed in spectral subset groups. If their respective distributions proved to be normal, their means were compared using a two-sided t Test [17] where the null hypothesis states that their means are equivalent. If their respective distributions did not adhere to normality, a two-sided Mann Whitney Wilcoxon Test [24] was used. This test is non-parametric alternative to the t Test that does not require an assumption normally distributed data. It's null hypothesis states that the two populations are equivalent in that they are sampled from populations with identical medians.

3. Results

3.1. Data

The field data representing the Single Variety dataset (Russet Norkotah) consisted of 242 instances that were evenly split between "Infected" and "Not Infected" classes and are detailed by Griffel et al. [12]. The greenhouse data making up the Multiple Varieties dataset yielded 422 instances evenly split between "Infected" and "Not Infected" classes. Additionally, 29 different breeding lines were represented in the data with smallest group consisting of 4 total instances and the largest group consisting of 32 total instances–all split evenly between "Infected" and "Not Infected". The spectral subsets for each dataset were plotted for visual assessment and shown in Fig. 4.

3.2. ANN modelling

The ANN modelling framework was successfully applied to each dataset's spectral subset for 100 iterations yielding sample populations ($n = 100$) for accuracy, precision, and recall derived from model testing and evaluation. Table 2 shows the descriptive statistics of the modelling outcomes.

Table 3
Results of the Shapiro-Wilks Test for normality.

Data	Spectral Subset	Acc. p-value	Prec. p-value	Recall p-value
Single Variety	380–720	6E-13	8E-10	2E-07
	500–900	5E-03	2E-02	3E-03
	720–900	2E-02	3E-02	3E-04
	720–1300	2E-04	7E-04	9E-04
	900–1300	7E-03	*2E-01	9E-05
Multiple Varieties	380–720	*1E-01	1E-11	9E-04
	500–900	*7E-02	3E-09	2E-02
	720–900	*6E-02	4E-07	1E-04
	720–1300	1E-02	1E-04	7E-07
	900–1300	1E-02	1E-07	4E-06

*Cannot reject H0 at a 0.95 confidence level.

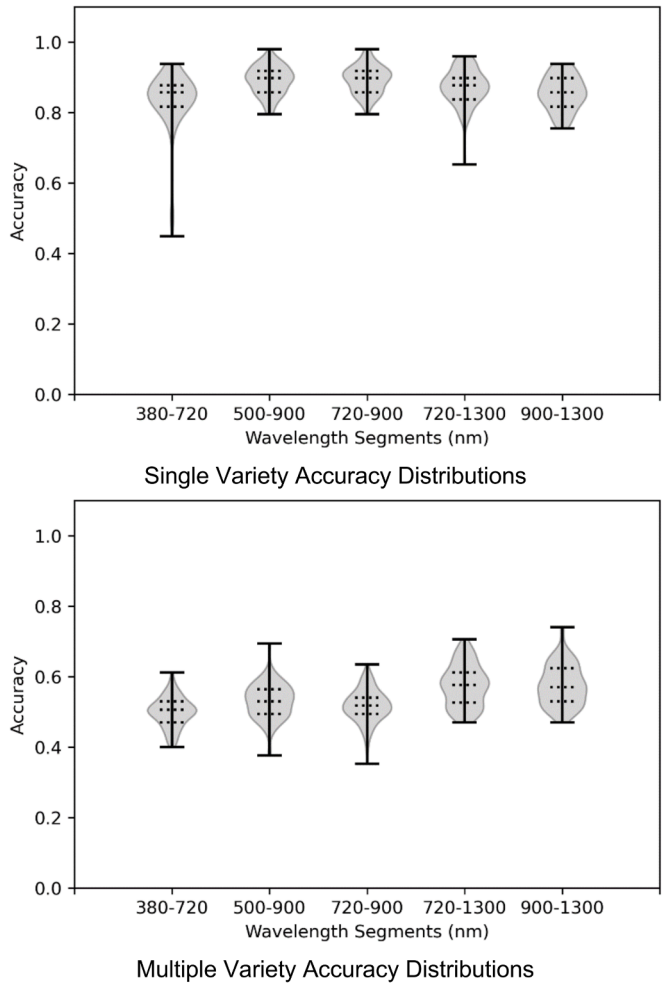

Fig. 6. Violin plots showing the accuracy distributions derived from ANN model testing for each spectral subset iteration group for the Single Variety and Multiple Varieties spectral datasets. The solid lines mark the minimum and maximum values of the distributions, and the dotted lines mark the 25th, 50th, and 75th quantiles.

Fig. 5 shows some examples of individual model training and validation data accuracy and loss metrics during training to provide visual reference of ANN validation training profiles.

3.3. Statistical analysis

The results of the Shapiro-Wilks Test for each modelling group are shown in Table 3. In the Single Variety segment, only one precision distribution from the 900–1300 nm spectral subset could be deemed normal as the returned probability value was not sufficient to reject H_0. In the Multiple Variety data, three accuracy distributions (spectral subsets 380–720 nm, 500–900 nm, and 720–900 nm) were also shown to be normally distributed. Based on these results, only results of the non-parametric statistical tests that do not require an assumption of normally distributed data will be presented.

The Kruskal-Wallis Test was applied to the model accuracy distribution groups for each dataset to determine if the spectral subsets were equivalent from the perspective of potentially having been drawn from the same population with the same median. Analysis of the Single Variety and Multiple Varieties datasets returned p-values of 4.25E-14 and 2.80E-26 respectively which are less than the threshold of 0.05 needed for the null hypothesis to remain valid. Therefore, the tests indicate that the modelling accuracy results among the spectral subsets in the Single Variety and Multiple Variety datasets are not equal and require additional post-hoc testing to identify which subset accuracy distributions are statistically different. Fig. 6 shows violin plots of the individual spectral subset ANN model accuracy distributions for the Single Variety and Multiple Varieties data. These provide a visual reference of both the size and shape of the accuracy distributions produced from the model iterations in the modelling framework.

The results of the post-hoc pair-wise Dunn's Test on the Single Variety and Multiple Varieties accuracy distributions by spectral subset are shown in Table 4. Among the spectral subset groups of the Single Variety data, the results indicate statistical differences exist among six of the possible 10 pairing options. Among the 10 possible pairs of the spectral subset groups within the Multiple Varieties dataset, all but three appear to be statistically different.

The results of the two-sided Mann Whitney Wilcoxon Tests performed on the precision and recall distributions derived from the ANN modelling iterations for each spectral subset are shown in Table 5. For this test, a p-value less than the threshold of 0.05 indicates the null hypothesis of equivalence must be rejected. Within the Single Variety

Table 4
Results of the post-hoc pair-wise Dunn's Test on model accuracy distributions of spectral subsets within the Single Variety and Multiple Varieties datasets.

Pairs	p-value (Single Variety)	p-value (Multiple Varieties)
(380–720)–(500–900)	5E-09	4E-04
(380–720)–(720–900)	8E-10	*2E-01
(380–720)–(720–1300)	3E-03	1E-17
(380–720)–(900–1300)	*1E+00	2E-18
(500–900)–(720–900)	*1E+00	*9E-01
(500–900)–(720–1300)	*1E-01	2E-05
(500–900)–(900–1300)	3E-06	9E-06
(720–900)–(720–1300)	5E-02	1E-09
(720–900)–(900–1300)	7E-07	4E-10
(720–1300)–(900–1300)	*1E-01	*1E+00

*Cannot reject H0 at a 0.95 confidence level.

Table 5
Results of the Mann Whitney Wilcoxon Test to test for precision and recall equivalence generated by the ANN modelling iterations for each spectral subset.

Data	Spectral Subsets	p-value
Single Variety	380–720	3E-06
	500–900	1E-02
	720–900	*5E-01
	720–1300	*2E-01
	900–1300	3E-02
Multiple Varieties	380–720	*8E-01
	500–900	3E-03
	720–900	2E-06
	720–1300	1E-04
	900–1300	3E-09

*Cannot reject H_0 at a 0.95 confidence level.

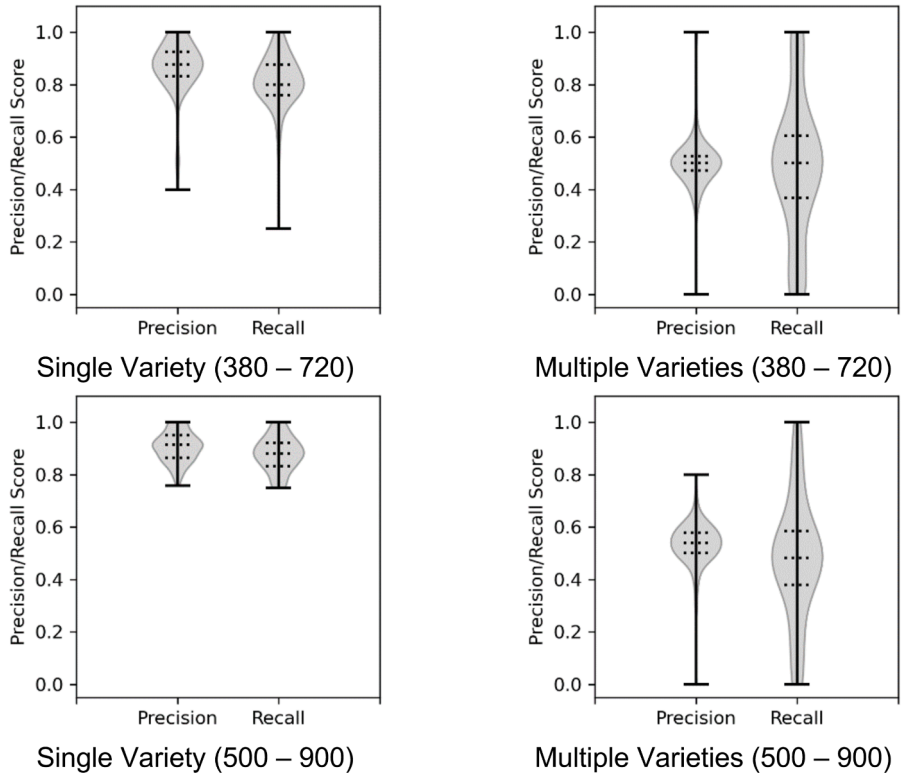

Fig. 7. Violin plots showing distributions of each pair of precision and recall distributions tested for equivalence. The solid lines mark the minimum and maximum values of the distributions, and the dotted lines mark the 25th, 50th, and 75th quantiles.

dataset, ANN modelling yielded precision and recall distributions with medians that do not statistically differ for the 720–900 nm and 720–1300 nm spectral subsets. Within the Multiple Varieties dataset, the results indicate precision and recall are not statistically different for the 380–720 nm spectral subset.

Fig. 7 shows violin plots for each precision and recall distribution tested for equivalence within the spectral subset groups.

4. Discussion

This analysis depended on spectral data collected and introduced by Griffel et al. [12] and on new spectral data collected at the USDA-ARS Small Grains and Potato Germplasm Research greenhouse facility in Aberdeen, Idaho, United States. With these data, researchers were able to evaluate ANN modelling performance for classification of potato foliage infected with PVY from non-infected counterparts using spectral datasets collected from a single variety and from multiple potato varieties. Although these data were collected in different environments and years, the methods to account for changes in lighting conditions and other factors that could potentially add bias were employed to allow for reasonable comparisons. The spectral subset plots shown in Fig. 4 provide a visual comparison of the Single Variety and Multiple Varieties datasets. Graphical assessment indicates that it is difficult to visually differentiate spectral curves collected from potato plants infected with or without PVY for any of the spectral subsets in the Multiple Varieties data. However, the Single Variety dataset shows more visual differentiation for all but the 380–720 spectral subset.

Overall, ANN model performance between the Single Variety and Multiple Varieties data were noticeably different as shown in Table 2. For the Single Variety data, the mean spectral subset classification accuracies ranged from 0.837 to 0.894. The mean spectral subset classification accuracies for the Multiple Varieties data ranged from 0.500 to 0.575, barely outperforming a baseline “guesser”. This is in line with observations by [7,18,34] that have documented that foliage symptoms vary between different potato varieties when infected with PVY. Although [2] showed promising results to detect PVY spectral profiles in potato foliage on four varieties, that is likely not an adequate comparison to this analysis since the Multiple Varieties dataset represented 29 different breeding lines. Additionally, MacKenzie et al. [23] documented differing PVY foliage symptoms based on viral strain and potato variety dynamics. These outcomes indicate an ANN model trained on and tasked with classifying PVY-infected potato plants based on spectral features for a single variety will likely outperform a counterpart trying to learn and infer on spectral data from a multitude of potato varieties without any context of the varietal heterogeneity within the feature space. Evidence of this also exists in the model accuracy and loss training patterns. Fig. 5 shows examples of ANN model validation accuracy and loss curves developed during training. The patterns produced by the ANN model learning on the Single Variety training data indicate the model was able to learn patterns within the spectral feature space to achieve highly accurate classification outcomes. Conversely, the rough and inconsistent accuracy and loss curves indicate the model training on data derived from the Multiple Varieties dataset appears to have struggled to discriminate suitable patterns from the spectral data feature space to achieve a reasonable classification accuracy.

Although ANN model testing data appear to show variations in testing performance, it was important to generate sample populations with which to apply robust statistical analysis to understand the impacts of subsetting spectral regions. This is intended to help inform future research efforts to identify important spectral wavelengths, especially when spectral resolutions are potentially limited by instrumentation. This iterative approach utilizing the ANN modelling framework developed for this analysis generated distributions representing ANN model testing performance for accuracy, precision, and recall that, in most cases, were shown to violate the normality assumption. This guided the selection of the statistical tests to verify that model performance did vary

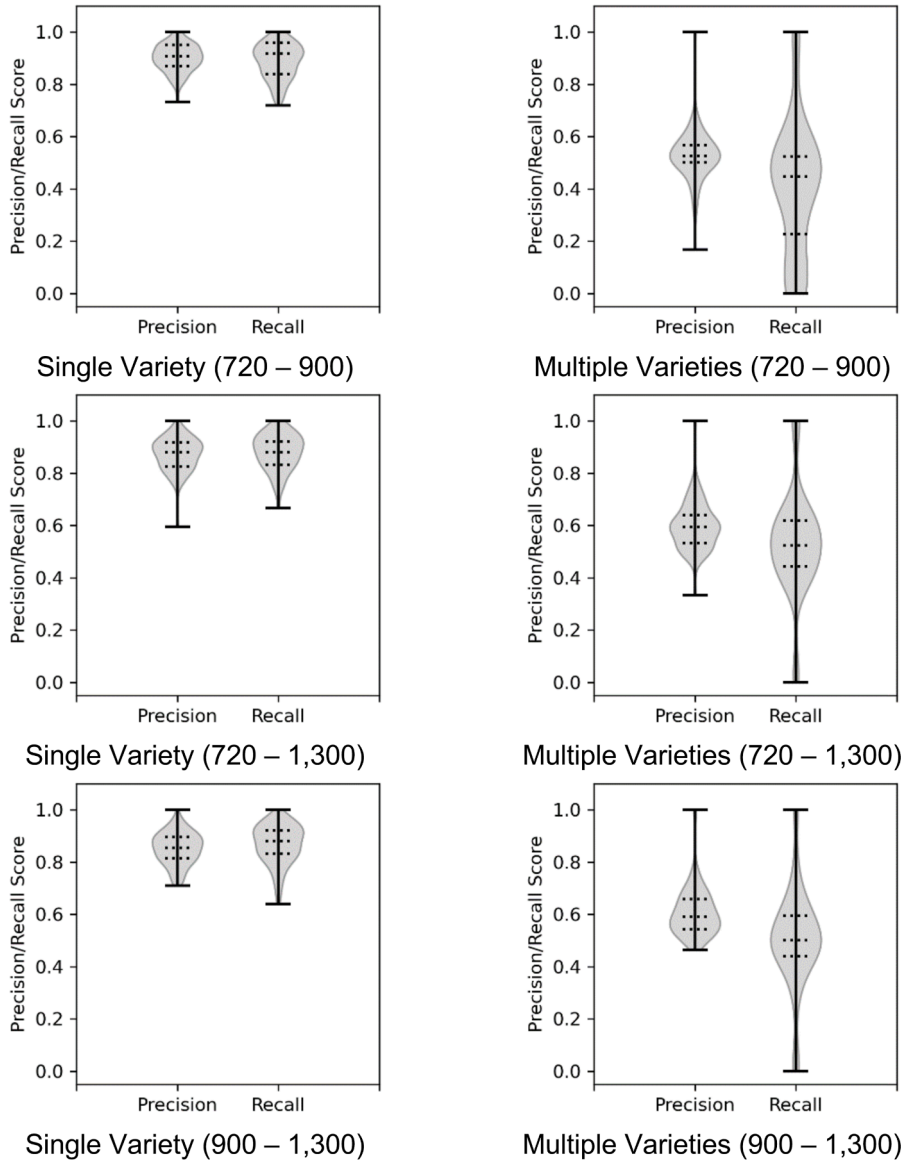

Fig. 7. (*continued*).

among the spectral subset groups for the Single Variety and Multiple Variety data. Based on this, the analysis indicates that spectral subsets identified by [12] do impact ANN classification accuracy when classifying on single or multiple varieties. It is important to note that the spectral ranges of 500–900 nm, 720–900 nm, and 720–1300 nm yielded the best accuracy performance metrics for the Single Variety data. This is in line with findings documented by [12, 32]. However, the ANN models did surpass the accuracy for the 380–720 nm spectral range documented by Griffel et al. [12]. The spectral ranges of 720–900 nm and 720–1300 nm yielded the highest classification accuracies for the Multiple Varieties data. However, given that these metrics were marginally higher than 0.50, it would be difficult to state that the ANN model achieved even adequate performance metrics.

Although classification accuracy is an important metric when assessing ANN model performance, precision and recall are also important, especially when trying to understand a potential bias toward false positive or false negative outcomes. For the Single Variety data, this analysis indicates that precision and recall did not vary for the 720–900 nm and 720–1300 nm spectral subsets, which also achieved the highest classification accuracies. However, ANN models utilizing the 500–900 nm spectral subset did yield a statistically higher precision metric indicating a slight bias toward false negative inferences. For the Multiple Varieties data, all ANN models except those utilizing the 380–720 produced statistically different metrics favoring precision.

5. Conclusion

This research shows that ANNs can achieve high classification accuracies to differentiate potato plants infected with PVY from non-infected counterparts and is in line with previous efforts. However, it is also apparent that an overarching classifier incorporating multiple potato plant varieties may not be successful and that varietal information does impact spectral features across all wavelengths evaluated in this analysis. Differing spectral regions appear to contain feature information that can impact ANN model performance and these methods support the concept of detecting PVY-infected potato plants in larger field areas based on specific spectral features. It is important to acknowledge that these data are limited and that more work is needed to expand spectral libraries to continue this type of research.

Declaration of Competing Interests

The authors declare that they have no known competing financial interests or personal relationships that could have appeared to influence the work reported in this paper.

Acknowledgements

We would like to thank all authors of consulted works, agricultural partners, and industry experts that provided technical guidance. We would also like to thank staff at the United States Department of Agriculture Agricultural Research Service (USDA-ARS) Small Grains and Potato Germplasm Research facility in Aberdeen, Idaho, United States. This research was funded by the Idaho Specialty Crop Block Grant Program (Grant Award numbers: 61150 / SPEC21, ISDA-1500-22A), Higher Education Research Council Idaho Global Entrepreneurial Mission Initiative and AmericaView through U.S. Geological Survey under Grant/Cooperative Agreement No. G18AP00077.

References

[1] Abadi, M., Agarwal, A., Barham, P., Brevdo, E., Chen, Z., Citro, C., Corrado, G.S., Davis, A., Dean, J., Devin, M., Ghemawat, S., Goodfellow, I., Harp, A., Irving, G., Isard, M., Jia, Y., Jozefowicz, R., Kaiser, L., Kudlur, M., Levenberg, J., Mane, D., Monga, R., Moore, S., Murray, D., Olah, C., Schuster, M., Shlens, J., Steiner, B., Sutskever, I., Talwar, K., Tucker, P., Vanhoucke, V., Vasudevan, V., Viegas, F., Vinyals, O., Warden, P., Wattenberg, M., Wicke, M., Yu, Y., Zheng, X., 2016. TensorFlow: large-scale machine learning on heterogeneous distributed systems.

[2] J.J. Couture, A. Singh, A.O. Charkowski, R.L. Groves, S.M. Gray, P.C. Bethke, P. A. Townsend, Integrating Spectroscopy with potato disease management, Plant Dis. 102 (2018) 2233–2240, https://doi.org/10.1094/PDIS-01-18-0054-RE.

[3] R.D. Davidson, A.J. Houser, K. Sather, R. Haslar, Controlling PVY in seed: what works and what does not, Am. J. Potato Res. 90 (2013) 28–32, https://doi.org/10.1007/s12230-012-9290-z.

[4] A. Devaux, P. Kromann, O. Ortiz, Potatoes for sustainable global food security, Potato Res. 57 (2014) 185–199, https://doi.org/10.1007/s11540-014-9265-1.

[5] A. Dinno, Nonparametric pairwise multiple comparisons in Independent Groups using Dunn's Test, Stata. J. 15 (2015) 292–300, https://doi.org/10.1177/1536867X1501500117.

[6] T.F. Döring, J. Schrader, C. Schüler, Representation of potato virus Y control strategies in current and past extension literature, Potato Res. 49 (2006) 225–239, https://doi.org/10.1007/s11540-007-9019-4.

[7] M.D. Draper, J.S. Pasche, N.C. Gudmestad, Factors influencing PVY development and disease expression in three potato cultivars, Am. J. Potato Res. 79 (2002) 155–165, https://doi.org/10.1007/BF02871931.

[8] F. Gao, S. Kawakubo, S.Y.W. Ho, K. Ohshima, The evolutionary history and global spatio-temporal dynamics of potato virus Y, Virus Evol. 6 (2020), https://doi.org/10.1093/ve/veaa056.

[9] M.W. Gardner, S.R. Dorling, Artificial neural networks (the multilayer perceptron)—a review of applications in the atmospheric sciences, Atmos. Environ. 32 (1998) 2627–2636, https://doi.org/10.1016/S1352-2310(97)00447-0.

[10] Glorot, X., Bordes, A., Bengio, Y., 2011. Deep sparse rectifier neural networks, in: Gordon, G., Dunson, D., Dudík, M. (Eds.), Proceedings of the Fourteenth International Conference on Artificial Intelligence and Statistics, Proceedings of Machine Learning Research. PMLR, Fort Lauderdale, FL, USA, pp. 315–323.

[11] S. Gray, S. de Boer, J. Lorenzen, A. Karasev, J. Whitworth, P. Nolte, R. Singh, A. Boucher, H. Xu, Potato virus Y: an evolving concern for potato crops in the United States and Canada, Plant Dis. 94 (2010) 1384–1397, https://doi.org/10.1094/PDIS-02-10-0124.

[12] L.M. Griffel, D. Delparte, J. Edwards, Using support vector machines classification to differentiate spectral signatures of potato plants infected with potato virus Y, Comput. Electron. Agricul. 153 (2018) 318–324, https://doi.org/10.1016/j.compag.2018.08.027.

[13] D.A. Halterman, A.O. Charkowski, J. Verchot, Potato, viruses, and seed certification in the USA to provide healthy propagated tubers. Pest Technology, 2012, pp. 1–14.

[14] D.C. Hane, P.B. Hamm, Effects of seedborne potato virus Y infection in two potato cultivars expressing mild disease symptoms, Plant Dis. 83 (1999) 43–45, https://doi.org/10.1094/PDIS.1999.83.1.43.

[15] R. Harrington, N. Katis, R.W. Gibson, Field assessment of the relative importance of different aphid species in the transmission of potato virus Y, Potato Res 29 (1986) 67–76, https://doi.org/10.1007/BF02361982.

[16] W. Haynes, Tukey's Test, in: Werner Dubitzky, O Wolkenhauer, H CK, H Y (Eds.), Encyclopedia of Systems Biology, Springer New York, New York, NY, 2013, pp. 2303–2304, https://doi.org/10.1007/978-1-4419-9863-7_1212.

[17] Kalpić Damir, N. Hlupić, M. L, Student's t-Tests, in: M Lovric (Ed.), International Encyclopedia of Statistical Science, Springer Berlin Heidelberg, Berlin, Heidelberg, 2011, pp. 1559–1563, https://doi.org/10.1007/978-3-642-04898-2_641.

[18] A.v Karasev, S.M. Gray, Continuous and emerging challenges of potato virus Y in potato, Annu. Rev. Phytopathol. 51 (2013) 571–586, https://doi.org/10.1146/annurev-phyto-082712-102332.

[19] J. Kaufmann, A.G. Schering, Analysis of variance ANOVA. Wiley StatsRef: Statistics Reference Online, American Cancer Society, 2014, https://doi.org/10.1002/9781118445112.stat06938.

[20] Kingma, D.P., Ba, J., 2017. Adam: a method for stochastic optimization.

[21] W.H. Kruskal, W.A. Wallis, Kruskal-Wallis Test. The Concise Encyclopedia of Statistics, Springer, New York, 2008, pp. 288–290, https://doi.org/10.1007/978-0-387-32833-1_216.

[22] K. Lindner, F. Trautwein, A. Kellermann, G. Bauch, Potato virus Y (PVY) in seed potato certification, J. Plant Dis. Protect. 122 (2015) 109–119.

[23] T.D.B. MacKenzie, X. Nie, V. Bisht, M. Singh, Proliferation of recombinant PVY Strains in two potato-producing Regions of Canada, and symptom expression in 30 important potato varieties with different PVY strains, Plant Dis. 103 (2019) 2221–2230, https://doi.org/10.1094/PDIS-09-18-1564-RE.

[24] P.E. McKnight, J. Najab, Mann-Whitney U Test. The Corsini Encyclopedia of Psychology, American Cancer Society, 2010, p. 1, https://doi.org/10.1002/9780470479216.corpsy0524.

[25] A.F.S. Mello, R.A. Olarte, S.M. Gray, K.L. Perry, Transmission efficiency of potato virus Y strains PVYO and PVYN-Wi by five aphid species, Plant Dis. 95 (2011) 1279–1283, https://doi.org/10.1094/PDIS-11-10-0855.

[26] E.J. Milton, M.E. Schaepman, K. Anderson, M. Kneubühler, N. Fox, Progress in field spectroscopy, Remote Sens. Environ. 113 (2009) S92–S109, https://doi.org/10.1016/j.rse.2007.08.001.

[27] P. Mishra, C.M. Pandey, U. Singh, A. Gupta, C. Sahu, A. Keshri, Descriptive statistics and normality tests for statistical data, Ann. Card. Anaesth. 22 (2019) 67–72, https://doi.org/10.4103/aca.ACA_157_18.

[28] S. Mondal, Y.-.H. Lin, J.E. Carroll, E.J. Wenninger, N.A. Bosque-Pérez, J. L. Whitworth, P. Hutchinson, S. Eigenbrode, S.M. Gray, Potato virus Y transmission efficiency from potato infected with single or multiple virus strains, Phytopathology® 107 (2017) 491–498, https://doi.org/10.1094/PHYTO-09-16-0322-R.

[29] S. Mondal, E.J. Wenninger, P.J.S. Hutchinson, M.A. Weibe, S.D. Eigenbrode, N. A. Bosque-Pérez, Contribution of noncolonizing aphids to potato virus Y prevalence in potato in Idaho, Environ. Entomol. 45 (2016) 1445–1462, https://doi.org/10.1093/ee/nvw131.

[30] S. Mondal, E.J. Wenninger, P.J.S. Hutchinson, J.L. Whitworth, D. Shrestha, S. D. Eigenbrode, N.A. Bosque-Pérez, Comparison of transmission efficiency of various isolates of Potato virus Y among three aphid vectors, Entomol. Exp. Appl. 158 (2016) 258–268, https://doi.org/10.1111/eea.12404.

[31] S. Mondal, W.M. Wintermantel, S. Gray, Infection dynamics of potato virus Y isolate combinations in three potato cultivars, Plant Dis. (2022), https://doi.org/10.1094/PDIS-09-21-1980-RE.

[32] C. Moslemkhani, F. hassani, E. Nasrollahi Azar, F. Khelgatibana, Potential of spectroscopy for discrimination of PVY infected potato from healthy plants, J. Crop Protect. 8 (2019) 143–151.

[33] P. Nolte, J. Miller, K.M. Duellman, A.J. Gevens, E. Banks, Disease Management, in: J.C. Stark, M. Thornton, P. Nolte (Eds.), Potato Production Systems, Springer International Publishing, Cham, 2020, pp. 203–257, https://doi.org/10.1007/978-3-030-39157-7_9.

[34] P. Nolte, J.L. Whitworth, M.K. Thornton, C.S. McIntosh, Effect of seedborne potato virus Y on performance of russet Burbank, Russet Norkotah, and Shepody potato, Plant Dis. 88 (2004) 248–252, https://doi.org/10.1094/PDIS.2004.88.3.248.

[35] R.G. Novy, J.L. Whitworth, J.C. Stark, B.L. Schneider, N.R. Knowles, M.J. Pavek, L. O. Knowles, B.A. Charlton, V. Sathuvalli, S. Yilma, C.R. Brown, M. Thornton, T. L. Brandt, N. Olsen, Payette Russet: a dual-purpose potato cultivar with cold-sweetening resistance, low acrylamide formation, and resistance to late blight and potato virus Y, Am. J. Potato Res. 94 (2017) 38–53, https://doi.org/10.1007/s12230-016-9546-0.

[36] R.L. Plaisted, D.E. Halseth, B.B. Brodie, S.A. Slack, J.B. Sieczka, B.J. Christ, K. M. Paddock, M.W. Peck, Eva: a midseason golden nematode- and virus-resistant variety for use as tablestock or chipstock, Am. J. Potato Res. 78 (2001) 65–68, https://doi.org/10.1007/BF02874826.

[37] G. Polder, P.M. Blok, H.A.C. de Villiers, J.M. van der Wolf, J. Kamp, Potato virus Y detection in seed potatoes using deep learning on hyperspectral images, Front. Plant. Sci. 10 (2019) 209.

[38] J. Rosenman, C.S. McIntosh, G.R. Aryal, P. Nolte, Planting a problem: examining the spread of seed-borne potato virus Y, Plant Dis. 103 (2019) 2179–2183, https://doi.org/10.1094/PDIS-11-18-2004-SR.

[39] K.-B.G. Scholthof, S. Adkins, H. Czosnek, P. Palukaitis, E. Jacquot, T. Hohn, B. Hohn, K. Saunders, T. Candresse, P. Ahlquist, C. Hemenway, G.D. Foster, Top 10 plant viruses in molecular plant pathology, Mol. Plant Pathol. 12 (2011) 938–954, https://doi.org/10.1111/j.1364-3703.2011.00752.x.

[40] K.M. Smith, F.T. Brooks, On the composite nature of certain potato virus diseases of the mosaic group as revealed by the use of plant indicators and selective methods of transmission, in: Proceedings of the Royal Society of London. Series B, Containing Papers of a Biological Character 109, 1931, pp. 251–267, https://doi.org/10.1098/rspb.1931.0080.

[41] N. Srivastava, G. Hinton, A. Krizhevsky, I. Sutskever, R. Salakhutdinov, Dropout: a simple way to prevent neural networks from overfitting, J. Mach. Learn. Res. 15 (2014) 1929–1958.

[42] M. Thornton, Potato growth and development, in: J.C. Stark, M. Thornton, P. Nolte (Eds.), Potato Production Systems, Springer International Publishing, Cham, 2020, pp. 19–33, https://doi.org/10.1007/978-3-030-39157-7_2.

[43] L. Torrance, M.E. Talianksy, Potato virus Y emergence and evolution from the andes of south america to become a major destructive pathogen of potato and other solanaceous crops worldwide, Viruses 12 (2020), https://doi.org/10.3390/v12121430.

[44] G. van Rossum, F.L. Drake, Python 3 Reference Manual, CreateSpace, Scotts Valley, CA, 2009.

[45] M. Verbeek, P.G.M. Piron, A.M. Dullemans, C. Cuperus, R.A.A. van der Vlugt, Determination of aphid transmission efficiencies for N, NTN and Wilga strains of Potato virus Y, Ann. Appl. Biol. 156 (2010) 39–49, https://doi.org/10.1111/j.1744-7348.2009.00359.x.

[46] P. Virtanen, R. Gommers, T.E. Oliphant, M. Haberland, T. Reddy, D. Cournapeau, E. Burovski, P. Peterson, W. Weckesser, J. Bright, S.J. van der Walt, M. Brett, J. Wilson, K.J. Millman, N. Mayorov, A.R.J. Nelson, E. Jones, R. Kern, E. Larson, C. J. Carey, İ. Polat, Y. Feng, E.W. Moore, J. VanderPlas, D. Laxalde, J. Perktold, R. Cimrman, I. Henriksen, E.A. Quintero, C.R. Harris, A.M. Archibald, A.H. Ribeiro, F. Pedregosa, P. van Mulbregt, A. Vijaykumar, A. Bardelli, pietro, A. Rothberg, A. Hilboll, A. Kloeckner, A. Scopatz, A. Lee, A. Rokem, C.N. Woods, C. Fulton, C. Masson, C. Häggström, C. Fitzgerald, D.A. Nicholson, D.R. Hagen, D. v Pasechnik, E. Olivetti, E. Martin, E. Wieser, F. Silva, F. Lenders, F. Wilhelm, G. Young, G.A. Price, G.-.L. Ingold, G.E. Allen, G.R. Lee, H. Audren, I. Probst, J. P. Dietrich, J. Silterra, J.T. Webber, J. Slavič, J. Nothman, J. Buchner, J. Kulick, J. L. Schönberger, J.V. de Miranda Cardoso, J. Reimer, J. Harrington, J.L. C. Rodríguez, J. Nunez-Iglesias, J. Kuczynski, K. Tritz, M. Thoma, M. Newville, M. Kümmerer, M. Bolingbroke, M. Tartre, M. Pak, N.J. Smith, N. Nowaczyk, N. Shebanov, O. Pavlyk, P.A. Brodtkorb, P. Lee, R.T. McGibbon, R. Feldbauer, S. Lewis, S. Tygier, S. Sievert, S. Vigna, S. Peterson, S. More, T. Pudlik, T. Oshima, T.J. Pingel, T.P. Robitaille, T. Spura, T.R. Jones, T. Cera, T. Leslie, T. Zito, T. Krauss, U. Upadhyay, Y.O. Halchenko, Y. Vázquez-Baeza, S. Contributors, SciPy 1.0: fundamental algorithms for scientific computing in Python, Nat. Methods 17 (2020) 261–272, https://doi.org/10.1038/s41592-019-0686-2.

[47] J.L. Whitworth, S.M. Gray, J.T. Ingram, D.G. Hall, Foliar and tuber symptoms of U. S. potato varieties to multiple strains and isolates of potato virus Y, Am. J. Potato Res. 98 (2021) 93–103, https://doi.org/10.1007/s12230-020-09820-1.

[48] J.L. Whitworth, R.G. Novy, D.G. Hall, J.M. Crosslin, C.R. Brown, Characterization of broad spectrum potato virus Y resistance in a solanum tuberosum ssp. andigena-derived population and select breeding clones using molecular markers, grafting, and field inoculations, Am. J. Potato Res. 86 (2009) 286–296, https://doi.org/10.1007/s12230-009-9082-2.

[49] R. Wijesinha-Bettoni, B. Mouillé, The Contribution of potatoes to global food security, nutrition and healthy diets, Am. J. Potato Res. 96 (2019) 139–149, https://doi.org/10.1007/s12230-018-09697-1.

[50] Y. Zeng, A.C. Fulladolsa, A. Houser, A.O. Charkowski, Colorado seed potato certification data analysis shows mosaic and blackleg are major diseases of seed potato and identifies tolerant potato varieties, Plant Dis. 103 (2018) 192–199, https://doi.org/10.1094/PDIS-03-18-0484-RE.